特別掲載

CALCULATION OF DOSE DISTRIBUTIONS IN RADIATION THERAPY BY A DIGITAL COMPUTER
I. THE COMPUTATION OF DOSE DISTRIBUTIONS IN A HOMOGENEOUS BODY FOR COBALT 60 γ-RAYS AND 4.3MV X-RAYS

By

Yoshio Onai, Toraji Irifune, and Teizo Tomaru
Department of Physics, Cancer Institute, Tokyo
Keisuke Konishi
Department of Radiology, Tokyo Medical and Dental University School of Medicine

デイジタル型電子計算機による線量分布の計算
第1報　コバルト60 γ線および4.3 MV X線の均質体内線量分布の計算

癌研究会癌研究所第6研究室（物理）
尾内　能夫，入船　寅二，都丸　禎三
東京医科歯科大学医学部放射線医学教室
小　西　　圭　介

（昭和42年7月8日受付）

最近，電子計算機を用いた線量計算法が数多く発表されているが，その大部分が標準の isodose chart をカードあるいはテープに記憶させて，これを電子計算機で加算する方法である．この方法はカードを作る作業が厄介であり，しかもそのカードにない照射野については計算できない．

Sterling は線量分布を表わす実験式を開発し，すべての照射野について任意の点の線量を計算できるようにした．しかし，この式は SSD 80cmの ^{60}Co 以外には適用できない．

我々は tissue-air ratio が照射野の power function で表わされることおよびすべての SSD についての深部量百分率がこのtissue-air ratio で表わせることを利用して，任意の矩形照射野およびSSDについて適用できる実験式を開発した．この方法は tissue-air ratio および中心軸の線量と軸外の線量の比即ち decrement value の数式化であって，計算値と実測値は大部分の点について3％以内の誤差である．

更に，斜入射の補正にも tissue-air ratio の概念を適用し，任意の形の均質体内の線量を計算できる一般式を導いた．

この式を用い，oval phantom について，斜入射照射，4門照射，120度振子照射および切線振子照射の線量分布を電子計算機で計算し，結果を直接線量分布図として print-out した．用いた計算機はGE 635および IBM 7090で一門当りの計算時間は約8秒である．

この研究は昭和40および41年度厚生省がん研究助成金によつて行われたものである．

Introduction

In recent years, several papers[1)8)11)13)14)16)21)-30)32)-35)] have been published on the application of the digital computers to automatic calculation of dose distributions in radiotherapy. Most of these methods

were based on the traditional isodose chart summing methods in which the isodose curves, obtained by actual measurements, were digitised by hand for different field sizes and stored on cards or tape. This hand-digitised method needs a great deal of preparatory work and limits calculations to those field sizes for which digitised values exist.

Recently, Sterling et al.[29] have derived a mathematical expression for the dose distributions of telecobalt with any field. From this formula, it is possible to compute conveniently depth dose at any point in any field. A disadvantage of this equation is that it is valid only for ^{60}Co sources used at 80 cm SSD. Since the source-skin distance varies throughout the rotation in moving field therapy, it is desirable to develop the formula which is applicable to any SSD.

In the present paper, a new mathematical expression for the dose distributions of ^{60}Co γ-rays and 4.3 MV X-rays, which is adaptable to any SSD and any rectangular field, is described. The method developed here is essentially a mathematical expression of the tissue-air ratio and decrement value.[18]

Mathematical Expression

The dose at any point can be obtained by the product of three factors; (1) a central axis depth dose, (2) a decrement value, which is the ratio of the dose at a point away from the central axis to the dose on the central axis at the same depth in the standard isodose curves, and (3) correction factors for an oblique incidence field, wedged field, and inhomogeneity. In this report, the factors (1) and (2), and for the oblique field of (3) are considered.

1. Cobalt 60 Gamma Rays

1. Percentage depth dose on the central axis

Pfalzner[20] has pointed out that the tissue-air ratio for ^{60}Co γ-rays may be expressed as a power function of the field area, in the form

$$TAR\ (d,\ A_d) = K\ (d)\ A_d^{m(d)} \quad \cdots\cdots(1)$$

where d is the depth below the skin surface,

A_d is the field area at the depth d,

K and m are constants for a given depth (and a given radiation quality), and

TAR is the tissue-air ratio for a depth d and field area A_d at that depth.

From this equation, he has derived that the central axis percentage depth dose may be expressed as

$$P_c\ (d, f, A_{do}) = 100\ \frac{K(d)}{K(d_o)} \left\{\frac{f+d_o}{f+d}\right\}^{2-2m(d)} A_{do}^{\ m(d)-m(do)} \quad \cdots\cdots(2)$$

where f is the source-skin distance, SSD,

d_o is the depth of the peak absorbed dose, and

P_c is the central axis depth dose in percentage of dose at the depth d_o.

According to this equation, the central axis percentage depth doses at any SSD may be calculated by a computer provided that the parameters K and m are expressed as a mathematical formula.

The values of K and m were obtained with the aid of the digital computer, using the new values of the tissue-air ratios calculated by Gupta et al.[10] The calculations were based on least-squares solutions of the logarithmic form of relation (1) above, utilising as data the tissue-air ratio values for six field areas, i.e., 4 × 4, 6 × 6, 8 × 8, 10 × 10, 15 × 15, and 20 × 20 cm.

It was found that the parameters K and m could be approximated by the method of least-squares,

in the range of $0.5 \leqq d \leqq 30$ cm by

$$K(d) = 1.00778 - 0.063527\ d + 0.0014216\ d^2 - 0.00001\ d^3 \quad \cdots\cdots(3)$$

$$m(d) = 0.01113 + 0.0070903\ d - 0.0000593\ d^2 \quad \cdots\cdots(4)$$

The results calculated by these formulae are shown in Table 1 in comparison with the original data obtained from the tissue-air ratios by Gupta et al. The tissue-air ratios and percentage depth doses calculated from equations (1) and (2), respectively, using equations (3) and (4), were compared with the tissue-air ratios published by Gupta et al., and the central axis percentage depth doses presented in Supplement No. 10 of the British Journal of Radiology. The results indicate that the errors are less than 3% as shown in Figs. 1 and 2.

Fig. 1. Comparison of calculated and experimental values of tissue-air ratio for ^{60}Co γ-rays. Solid line is the data taken from Gupta et al. Broken line is calculated from equation (1) using equations (3) and (4).

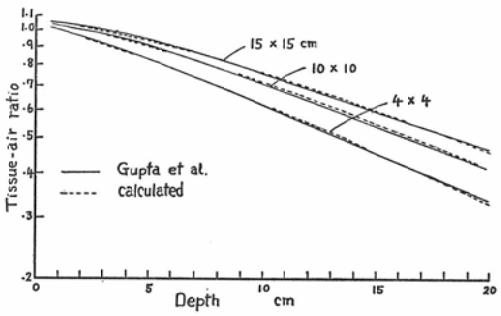

Fig. 2. Comparison of calculated and experimental values of percentage depth dose for ^{60}Co γ-rays. Solid line is the data taken from Brit. J. Radiol. Suppl. 10. Broken line is calculated from equation (2) using equations (3) and (4).

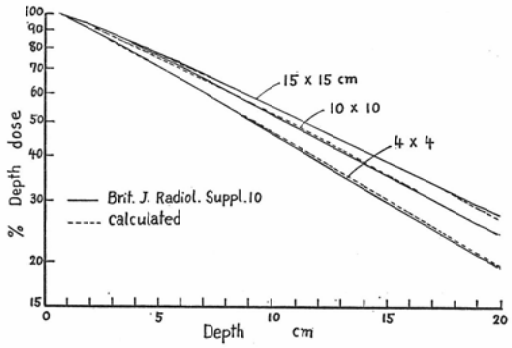

Equations (1) and (2) can be applied to any rectangular field provided that the field area A is expressed as an equivalent area, although the fields of equal areas but different shapes give rise to different percentage depth doses on the central axis.

The equivalent area A_e, which will have a smaller area than that of the rectangular field but the same percentage depth doses, is defined as

$$A_e = F_r A' \quad \cdots\cdots(5)$$

where A' is the actual area of the rectangular field, and

F_r is the area reduction factor.

Analysis of the central axis percentage depth doses for the rectangular field calculated by Clarkson's method[3] has shown that the area reduction factor may be expressed as (Fig. 3)

$$F_r = \frac{4E}{(1+E)^2} = \frac{4ab}{(a+b)^2} \quad \cdots\cdots(6)$$

where E is the elongation ratio, a/b, and

a and b are the major and minor axes of a rectangular field, respectively.

Substituting (6) into (5), we obtain

$$A_e = \left(\frac{2ab}{a+b}\right)^2 \quad \cdots\cdots(7)$$

This expression is equivalent to that of Sterling, in which the percentage depth doses for a rectangular

Fig. 3. Variation of area reduction factor with elongation ratio

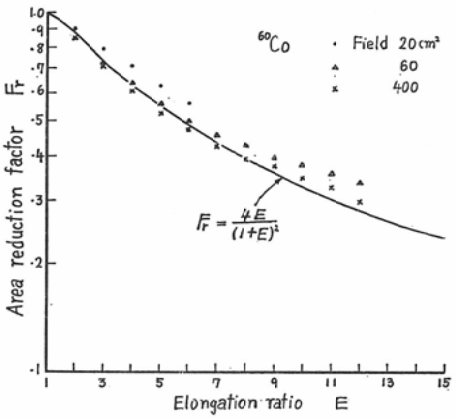

field are expressed as a function of (area/perimeter) of the field.

While d_o in equation (2) is defined as the depth of the peak absorbed dose, equation (2) may be valid for the depth dose in percentage of dose at any depth. Consequently, equation (2) becomes

$$P_c\ (d,\ f,\ A_{e,x_0}) = 100\frac{K(d)}{K(x_0)}\left\{\frac{f+x_0}{f+d}\right\}^{2-2m(d)} A_{e,x_0}^{\,m(d)-m(x_0)} \quad \cdots\cdots(8a)$$

or, substituting equation (7) for A_{e,x_0}, we find

$$P_c\ (d,\ f,\ A_{e,x_0}) = 100\frac{K(d)}{K(x_0)}\left\{\frac{f+x_0}{f+d}\right\}^{2-2m(d)}\left\{\frac{2ab}{a+b}\right\}_{x_0}^{2m(d)-2m(x_0)} \quad \cdots\cdots(8b)$$

where x_0 is the depth of the reference point,

A_{e,x_0} is the equivalent area at the reference point,

a and b are the major and minor axes, respectively, of a rectangular field at the reference point,

P_c is the central axis depth dose at the depth d in percentage of dose at the reference point x_0, and

d and f are the same as defined above,

This equation is useful for calculating the depth dose for fixed field therapy by means of a constant source-tumor distance, which is called the STD method and has been done with a rotation unit in our hospital since March 1957, and also is adaptable to rotation therapy by a slight modification. These further applications will be described later.

2. Percentage depth doses at points away from the central axis

The advantages of transverse data or decrement values for describing the dose distribution have been discussed by Orchard[18] and Orr et al.,[19] and a similar approach was used by Evans.[7] Onai et al.[17] have also reported that the method of Evans, in which the square field isodose crossplots have been used, may be applied with some modifications to the construction of isodose charts for any rectangular field without serious loss of accuracy from minimum experimental data. The isodose crossplot method is the most convenient for obtaining the standard isodose charts in manual work, but for the computer programme the method based on the decrement value may be more suitable.

Sterling et al. have shown that the relationship between the decrement value, k, and the ratio l/L, where L is half the field width at the surface and l is the distance of the intercept on the surface of the line joining the considered point Q to the source from the central axis (Fig. 4), may be approximated with good accuracy by a cumulative normal probability function and that the value of the function is

independent of the field size and its variation with depth is small.

The experimental investigations were carried out on the Toshiba RI-107 rotating unit with a 1.5-cm diameter source, collimated distance of 39 cm, and at both 60 and 50 cm SSD.

From the analysis of these data, it was found that the values of k were independent of the field size, as shown in Fig. 5, and depend on the depth in the umbra, as shown in Fig. 6. These relations were only slightly dependent on SSD and the shape of the rectangular field.

Fig. 4. Diagram showing symbols used in dosage calculations

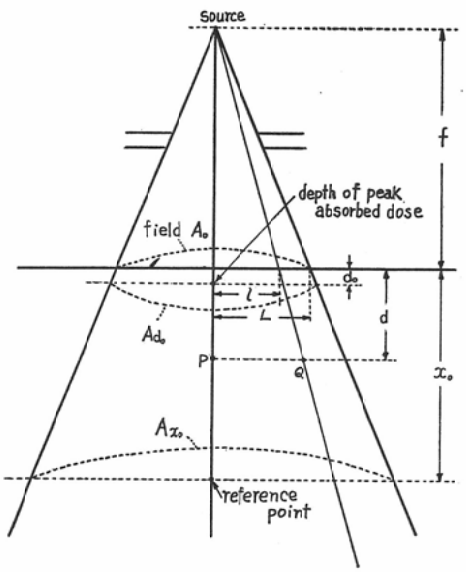

Fig. 5. Variation of decrement value k with (l/L—1) for ^{60}Co

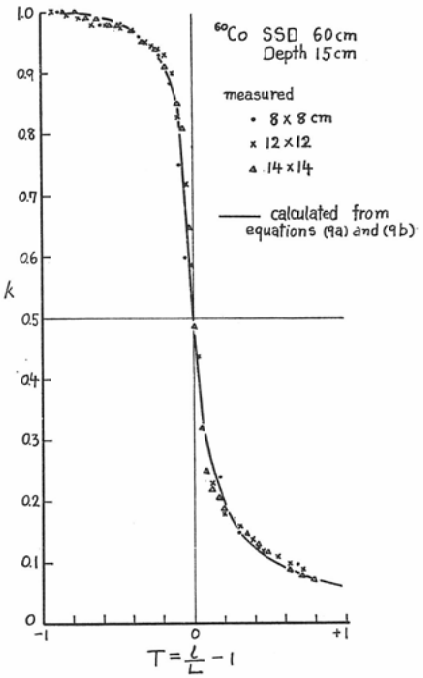

The relations between k and l/L may be expressed as follows. When $T \leqq O$ (i.e., inside the geometrical field), where $T=l/L-1$,

$$k=0.5\left\{2-\frac{1}{\{1.375+1.100(-T)+5.841(-T)^2\}^3-1.6e^{-2000(-T)^3}}\right\} \quad \cdots\cdots(9a)$$

and when $T \geqq O$ (i.e., outside the geometrical field)

$$k=\frac{1}{2+(5.93+9.16e^{1.272-0.0848d})T} \quad \cdots\cdots(9b)$$

From equations (8) and (9), the percentage depth dose P_Q at any point in the normal single field can be obtained by

$$P_Q\ (d, f, T, A_{e,x_0}) = k(d,T) \cdot Pc\ (d, f, A_{e,x_0}) \quad \cdots\cdots(10)$$

Calculated values from equations (9a) and (9b) are shown in Figs. 5 and 6 in comparison with experimental data. At the some values of l/L, the errors are greater than 10%, whereas the errors of displacement, which is expressed as the distance between the actual isodose point and calculated isodose point, are mostly within 1 mm. These errors may be neglected in clinical practice.

3. Correction for oblique field

Onai et al.[17] have reviewed three methods for deriving an isodose chart for oblique incidence from the normal incidence chart and recommended that the isodose curve shift method may be the simplest one in manual planning, but for the computer programme, the correction method using the tissue-air ratio may be more convenient.

In the case of oblique incidence, as shown in Fig. 7, the percentage depth dose at the point Q or Q′

Fig. 6. Variation of decrement value k with (l/L—1) for ^{60}Co

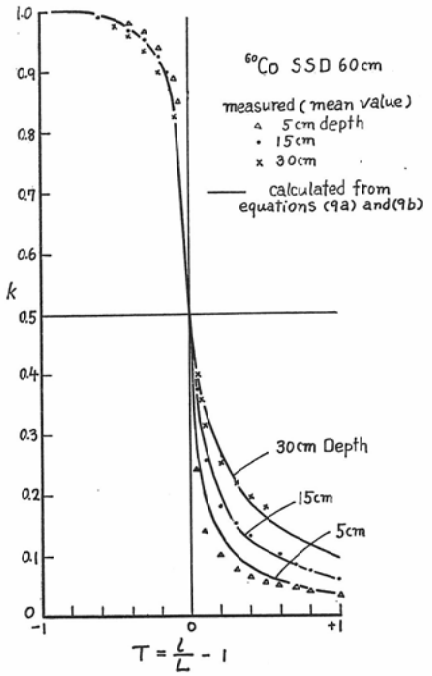

Fig. 7. Diagram showing notation in dosage calculation for oblique field

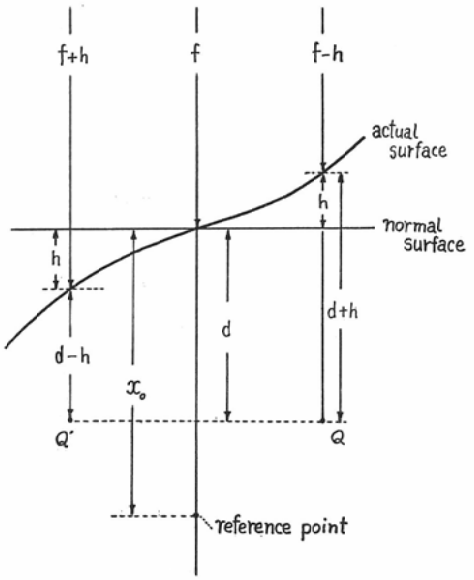

can be obtained by multiplying equation (10) by the tissue-air ratio correction factor T_r, where T_r is given by[6)31)]

$$T_r=\frac{K(d\pm h)\ A_{e,x_0}^{m(d\pm h)}}{K(d)\ A_{e,x_0}^{m(d)}}\left\{\frac{f+d}{f+x_0}\right\}^{2m(d\pm h)-2m(d)} \quad \cdots\cdots(11)$$

Then, equation (10) becomes

$$P_Q=100\ k\ (d,\ T)\frac{K(d\pm h)}{K(x_0)}\left\{\frac{f+x_0}{f+d}\right\}^{2-2m(d\pm h)} A_{e,x_0}^{m(d\pm h)-m(x_0)} \quad \cdots\cdots(12)$$

where the sign of h is appropriately chosen.

According to equation (12), the percentage depth doses at any point in a homogeneous body can be obtained whether the field is normal incidence or not.

II. 4.3 MV X-Rays

In principle, equation (12) can also be applied to the calculation of doses for 4.3 MV X-rays. To obtain the mathematical expressions for K, m, and k for 4.3 MV X-rays, experimental investigations were

carried out on a linear accelerator manufactured by Mullard Research Laboratories. The results may be expressed as follows.

The parameters K and m in the power law for tissue-air ratio may be approximated, in the range of $1.0 \leqq d \leqq 30$ cm, by

$$m(d) = 0.00081 + 0.0083966\ d - 0.00023696\ d^2 + 0.0000035224\ d^3 \quad \cdots\cdots(13)$$

$$K(d) = 1.07001 - 0.068230\ d + 0.0018682\ d^2 - 0.000020490\ d^3 \quad \cdots\cdots(14)$$

For the decrement value, when $T \leqq O$

Fig. 8. Comparison of calculated and measured values of tissue-air ratio for 4.3 MV X-rays. Solid line is the measured value. Broken line is calculated from equation (1) using equations (13) and (14).

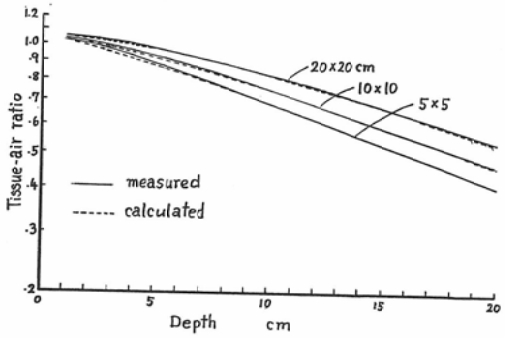

Fig. 9. Comparison of calculated and measured values of percentage depth dose for 4.3 MV X-rays. Solid line is the measured value. Broken line is calculated from equation (2) using equations (13) and (14).

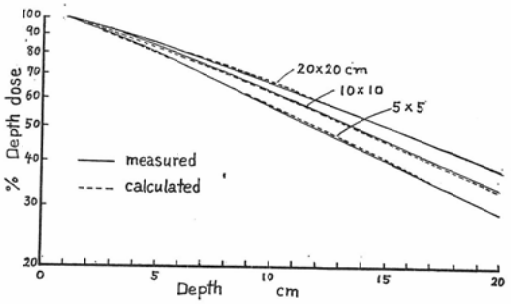

Fig. 10. Variation of decrement value k with (l/L—1) for 4.3 MV X-rays

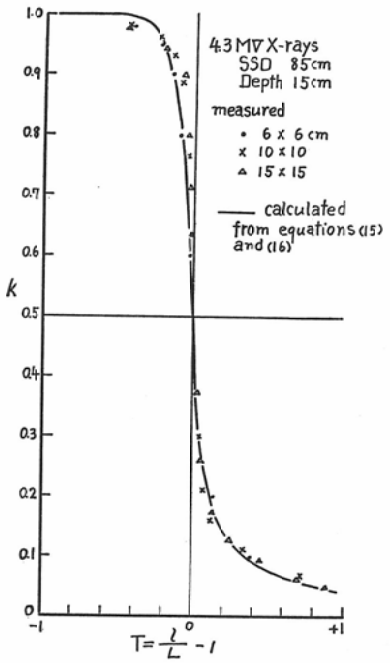

Fig. 11. Variation of decrement value k with (l/L—1) for 4.3 MV X-rays

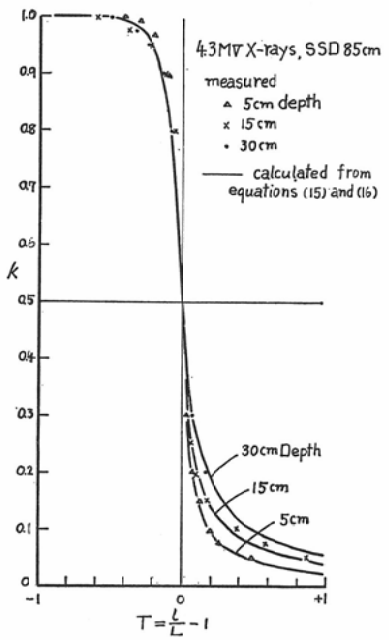

$$k=1-0.5e^{13.680T} \quad \cdots\cdots(15)$$

and when $T \geqq O$,

$$k=\frac{1}{2+(32.551-0.547d+0.454e^{4.95-0.33d})T} \quad \cdots\cdots(16)$$

Comparisons between the measured and calculated values from these equations are shown in Figs. 8,9,10, and 11. The accuracy is the same order as for ^{60}Co γ-rays.

Equation (7) for the equivalent area may also be adaptable to 4.3 MV X-rays.

Applications

1. Single field

Figs. 12 and 13 show an example of a single field for ^{60}Co γ-rays and 4.3 MV X-rays, respectively,

Fig. 12. Comparison of isodose distributions as plotted by computer and by measurements for ^{60}Co, with SSD 60cm and an 8 × 8 cm field at STD 75 cm. The printed degits are computed dose values and lines are measured isodose curves.

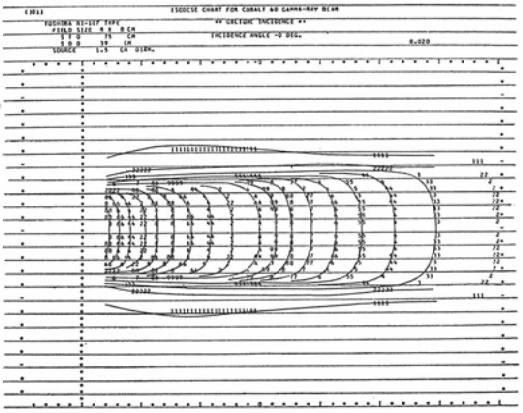

Dose	10	20	30	40	50	60	70	80	90	100
Symbol	1	2	3	4	5	6	7	8	9	A
Dose	120	140	160	180	200	220	240	260	280	300
Symbol	2	4	6	8	B	2	4	6	8	C

as plotted by the computer and compared with actual measurement. The printed digits are computed dose values and lines are the measured isodose curves. The point of 15 cm depth on the central axis is used as the reference point and printed by the symbol +, which is taken as 100 percent.

For the visualization of the dose distribution, a system of symbolic print-out is used by which a dose in the range of some percentage, indicated at the right shoulder in Figs. 12 and 13, that is 0.02 (2%), of a given percentage depth dose is printed in the same symbol and the dose is then printed as a symbol with the symbol table given at the bottom of Fig. 12. For instance, the point of symbol A expresses the dose of 100 ± 2 and symbol B the dose of 200 ± 4, etc.

In Fig. 14 is shown an example of an oblique incidence with an 8 × 8 cm field and surface obliquity of 30 degrees.

2. Multiple field

Fig. 15 shows an example of a multiple field, which is the resultant distribution obtained by com

Fig. 13. Comparison of isodose distributions as plotted by computer and by measurements for 4.3 MV X-rays, with SSD 85 cm and a 10× 10 cm field at STD 100 cm

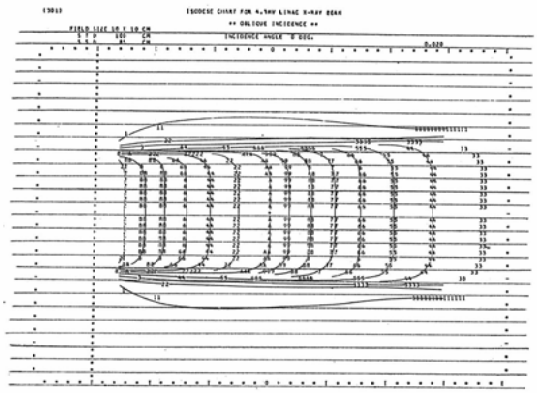

Fig. 14. Computer print out of the isodose distributions of an oblique incidence for ^{60}Co, with an 8 × 8 cm field at STD 75 cm and surface obliquity of 30 degrees

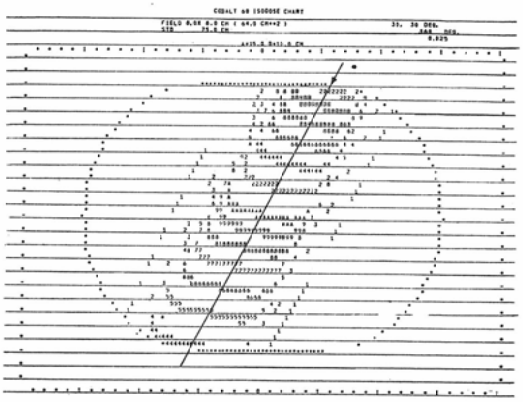

bining four ^{60}Co fields of area 6 × 15 cm at STD 75 cm arranged as two opposing pairs at 90 degrees to an oval phantom. Corrections for oblique incidence were made using equation (12).

3. Moving field

In rotation therapy, by dividing the patient's contour into a large number of segments as shown in Fig. 16 and considering the rotation as series of fixed radial fields over these segments, an approximation of the dose delivered at any point can be made.[9)15)] In general, since the body contour is not circular but roughly elliptical, as the patient rotates, the source to skin distance f_i, surface to axis distance x_i,

Table 1. Comparision of the values of m and K for ^{60}Co obtained from the new values of tissue-air ratio by Gupta et al. and calculated from equations (3) and (4)

Depth cm	from Gupta's data		from equations (3) & (4)	
	m	K	m	K
0.5	0.01454	0.97122	0.01466	0.97638
2	0.02630	0.88882	0.02507	0.88634
4	0.03851	0.78557	0.03854	0.77578
6	0.05081	0.68434	0.05154	0.67564
8	0.06407	0.58581	0.06405	0.58543
10	0.07599	0.50035	0.07610	0.50467
12	0.08775	0.42551	0.08767	0.43289
14	0.09897	0.36321	0.09877	0.36960
16	0.10956	0.31087	0.10939	0.31432
18	0.11853	0.26758	0.11954	0.26657
20	0.12897	0.22890	0.12921	0.22588
22	0.13854	0.19522	0.13841	0.19176
24	0.14759	0.16715	0.14713	0.16373
26	0.15545	0.14427	0.15538	0.14131
28	0.16542	0.12294	0.16316	0.12403
30	0.16852	0.10780	0.17046	0.11140

tissue depth d_i, and position of point within the field T_i will change from one position to the next. However, the source-axis distance, SAD ($F=f_i + x_i$), is constant. Consequently, it is convenient to express the dose at any point as a ratio of the air dose at the axis of rotation.

If the dose in air at the axis of rotation is denoted by $D_{c,a}$, the depth dose D_c at the axis of rotation is approximately given by

$$D_c / D_{c,a} = \sum_{i=1}^{n} TAR_i = \sum_i K(x_i) \cdot A_e^{m(x_i)} \qquad \cdots\cdots\cdots(17)$$

where x_i is the surface-axis distance for each position of the beam i, where i=1,2,3, ...n,

A_e is the field area at the axis of rotation.

The depth dose for other point P (in Fig. 16) can be obtained as follows.

The central axis depth dose at depth d_i for each field is given by

$$D_{d_i} = D_{c,a} \cdot K(d_i) \cdot A_e^{m(d_i)} \cdot \left\{\frac{f_i+x_i}{f_i+d_i}\right\}^{2-2m(d_i)} \qquad \cdots\cdots\cdots\cdots(18)$$

Fig. 15. Computer print-out of the isodose distributions for four 6 × 15 ^{60}Co fields at STD 75 cm arranged as two opposing pairs at right angles

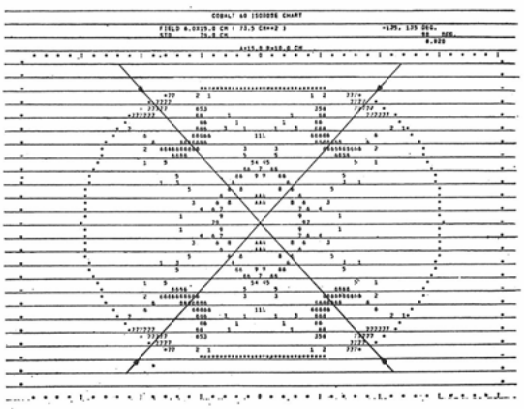

Fig. 16. Diagram showing notation in dosage calculation for moving field

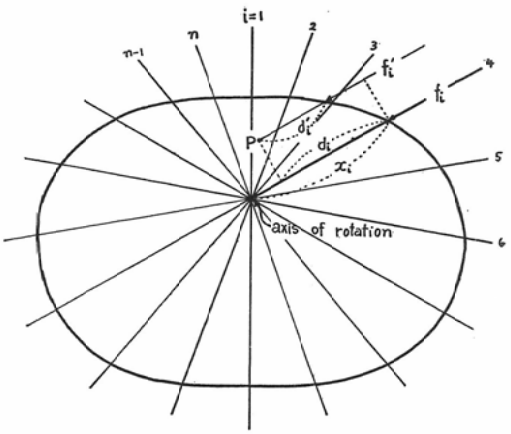

If the field is normal to the surface, the dose $D'_{p,i}$ at the point P may be expressed as

$$D'_{p,i} = D_{d_i} \cdot k(T_i, d_i) = D_{c,a} \cdot k(T_i, d_i) \cdot K(d_i) \cdot A_e^{m(d_i)} \cdot \left\{\frac{f_i+x_i}{f_i+d_i}\right\}^{2-2m(d_i)} \qquad \cdots\cdots(19)$$

Since the field is oblique incidence for the point P, by multiplying equation (19) by the tissue-air ratio correction factor (equation (11)) the actual dose $D_{p,i}$ at the point P for each field can be obtained, as

$$D_{p,i} = D'_{p,i} \cdot T_r = D_{c,a} \cdot k(T_i, d_i) \cdot K(d'_i) \cdot A_e^{m(d'_i)} \cdot \left\{\frac{f_i+x_i}{f_i+d_i}\right\}^{2-2m(d'_i)} \qquad \cdots\cdots(20)$$

where d'_i is the thickness of tissue between the point P and the surface measured along a line parallel to the central axis of the beam.

Since $f_i + d_i$ is equal to $f'_i + d_i'$, equation (20) becomes

$$D_{p,i} = D_{c,a} \cdot k(T_i, d_i) \cdot K(d_i') \cdot A_e^{m(d_i')} \cdot \left\{ \frac{f_i + x_i}{f_i' + d_i'} \right\}^{2-2m(d_i')} \quad \cdots\cdots\cdots(21)$$

The total dose delivered at the point P can be obtained by summing the dose for each field as $D_p = \sum_i D_{p,i}$

The summated doses may be expressed as a percentage of the total dose to the rotation center. That is,

$$P_p = 100\frac{D_p}{D_c} = \frac{\sum k(T_i, d_i) \cdot K(d_i') \cdot A_e^{m(d_i')} \cdot \left\{ \frac{F}{f_i' + d_i'} \right\}^{2-2m(d_i')}}{\sum K(x_i) \cdot A_e^{m(x_i)}} \quad \cdots\cdots(22)$$

where F is $f_i + x_i$, which is the source-axis distance.

Fig. 17 shows a computer print-out of dose distribution for a 120 degree-arc of a 6 × 15 cm field at the axis, which is obtained by the superimposition of 13 fields with entry angle at 10-degree intervals using equation (22). On the basis of the result by Haynes and Froese,[12] the body cross-section was expressed as

$$r = a - b \cos 2\theta \quad \cdots\cdots(23)$$

where $a = (A + B)/2$, $b = (A - B)/2$, and A and B are the semi-major and semi-minor axes of the body, respectively. In Fig. 17, 15 and 10 cm were used as A and B, respectively. Then the body cross-section was also printed out by the computer.

Since the dose distribution for rotation therapy is approximated by a series of fixed fields as described above, it is clear that the greater the number of fixed fields used in calculation, the more accurately is the dose distribution for moving field represented.

Considerations of the number of fields which needs to be summed in order to approximate to the true integrated dose have been carried out by Gregory,[9] Craig,[4] and Onai et al.[17] In general, no serious error is introduced by the use of summations at 15-degree intervals even in the low dose level, but errors may be significant in the particular cases such as a tangential rotation. The choice of the number of fields used in calculation, therefore, should be determined by the type of rotation, the size of field, and shape of body cross-section, etc.

Fig. 17. Computer print-out of the isodose distributions for a 120-degree arc of 6 × 15 cm ^{60}Co field at the rotation axis

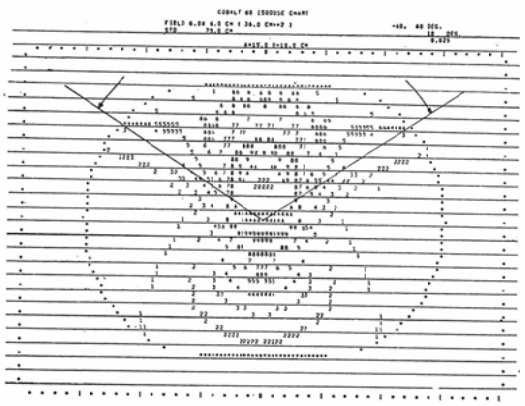

Fig. 18. Computer print-out of the isodose distributions for the tangential rotation calculated by the summation at 15-deg. intervals

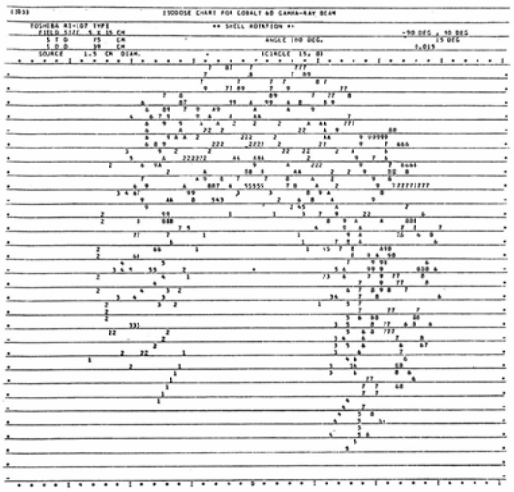

Fig. 19. Computer print-out of the isodose distributions for the tangential rotation calculated by the summation at 6-deg. intervals

Fig. 18 shows a computer print-out for the tangential rotation calculated by the summation at 15-deg. intervals. Fig. 19 shows the result by the summation at 6-deg. intervals. It can be seen that errors are significant both in the regions of low and high dose level.

The present programme is written in FORTRAN IV for a GE 635 digital computer. The length of time involved in calculation is eight seconds per field and may be taken for multiple or moving fields as long as time multiplying time per field by the number of fields used in calculation. A relatively small machine, such as the TOSBAC 3400, may take as long as 70 seconds per field.

Summary

A mathematical expression is presented for approximating the dose distributions in rectangular beams of ^{60}Co γ-rays and 4.3 MV X-rays in a water equivalent medium. This equation, supported by experimental results, may be used for any field, any SSD, and any oblique field, and can be used to print out the combined multifield isodose curves directly with small error. Examples of the computer print-out of a single field, oblique field, two opposing pairs, 120-deg. arc, and tangential rotation were shown.

Acknowledgments

This work has been supported by a research grant for cancer from the Ministry of Health and Welfare, which is gratefully acknowledged. The authors wish to express their thanks to Mr. Y. Kanno, senior programmer of the Tokyo Shibaura Electric Co., Ltd. of Kawasaki, for his continous and stimulating interest and for allowing so much time to be spent on this project.

REFERENCES

1) Bentley, R.E.: Digital computers in radiation treatment planning, Brit. J. Radiol. 37 (1964), 748—755.
2) Castro, V., Soifer, C., and Quimby, E.H.: Calculation of dosage in vertical rotation therapy using standard isodose charts, Amer. J. Roentgenol. 73 (1955), 815—826.
3) Clarkson, J.R.: A note on depth doses in fields of irregular shape, Brit. J. Radiol. 14 (1941), 265—268.
4) Craig, D.: Determination of dose in arc therapy by numerical integration, Brit. J. Radiol. 38 (1965), 285—287.
5) Depth dose tables for use in radiotherapy, Brit. J. Radiol. Supple. No. 10, 1961.

6) Du Sault, L.A., and Legare, J-M.: Dosage calculations for oblique beams of radiation, Radiology 80 (1963), 856—862.
7) Evans, E.A.: A method for construction of isodose charts from minimum experimental data, Amer. J. Roentgenol. 81 (1959), 24—29.
8) Fitzgerald, L.T., Bruno, F.P., and Mauderli, W.: An automatic depth-dose acquisition system, Radiology 86 (1966), 1107—1109.
9) Gregory, C.: Dosage distribution in rotational cobalt 60 therapy a simplified method of computation, Brit. J. Radiol. 30 (1957), 538—543.
10) Gupta, S.K., and Cunningham, J. R.: Measurement of tissue-air ratios and scatter functions for large field sizes, for cobalt 60 gamma radiation, Brit. J. Radiol. 39 (1966), 7—11.
11) Halldén, H., Ragnhult, I., and Roos, B.: Computer method for treatment planning in external radiotherapy, Acta Radiologica, Therapy, Physics, Biology, 1 (1963), 407—416.
12) Haynes, R.H., and Froese, G.: Idealized body contours in rotation dosimetry, Acta Radiologica 48 (1957), 209—226.
13) Hope, C.S., and Walters, J.H.: The computation of single and multiple field depth doses for 4 MV X-rays, Phys. Med. Biol. 9 (1964), 517—519.
14) Hope, C.S., and Orr, J.S.: Computer optimization of 4 MeV treatment planning, Phys. Med. Biol. 10 (1965), 365—373.
15) Jones, D.E.A., Gregory, C., and Birchall, I.: Dosage distribution in rotational cobalt 60 therapy, Brit. J. Radiol. 29 (1956), 196—201.
16) Mauderli, W., and Fitzgerald, L.T.: A computer progamme for automatic rotational treatment planning, Phys. Med. Biol. 9 (1964), 102—104.
17) Onai, Y., Tomaru, T., and Irifune, T.: Considerations on methods of constructing isodose curves from minimum experimental data. I, II, III, and IV, Nipp. Act. Radiol. (In press.)
18) Orchard, P.G.: Decrement lines: a new presentation of data in cobalt 60 beam dosimetry, Brit. J. Radiol. 37 (1964), 756—763.
19) Orr, J.S., Laurie, J., and Wakerley, S.: A study of 4 MeV transverse data and associated methods of constructing isodose curves, Phys. Med. Biol. 9 (1964), 505—515.
20) Pfalzner, P.M.: A general formula for axial depth dose derived from an empirical power law for tumour-air ratios, Radiology 75 (1960), 438—445.
21) Richter, J., und Schirrmeister, D.: Ein Verfahren zur Berechnung der Dosisverteilungen mit digitalen Rechenautomaten, Strahlenther. 123 (1964), 45—58.
22) Richter, J., und Schirrmeister, D.: Die Ermittlung von Dosisverteilungen mit digitalen Rechenautomaten unter Berücksichtigung von Randabfall und Streuung, Strahlenther. 126 (1965), 177—184.
23) Richter, J., und Schirrmeister, D.: Die Berücksichtigung von Gewebeinhomogenitäten bei der Ermittlung von Dosisverteilungen mit digitalen Rechenautomaten, Strahlenther. 127 (1965), 550—559.
24) Schirrmeister, D., und Richter, J.: Die Berechnung von Dosisverteilungen mit digitalen Rechenautomaten bei mehraxialer Pendelbestrahlung, Strahlenther. 125 (1964), 211—218.
25) Schoknecht, G.: Berechnung und Ausdrucken von Dosisverteilungen für die Co-60-Teletherapie mit dem Datenverarbeitungssystem IBM 1401 nach experimentell bestimmten Ausgangswerten, Strahlenther. 125 (1964), 75—90.
26) Sterling, T.D., Perry, H., and Bahr, G.K.: A practical procedure for automating radiation treatment planning, Brit. J. Radiol. 34 (1961), 726—733.
27) Sterling, T.D., Perry, H., and Weinkam, J.J.: Automation of radiation treatment planning. II. Calculation of non-convergent field dose distributions, Brit. J. Radiol. 36 (1963), 63—67.
28) Sterling, T.D., Perry, H., and Weinkam, J.J.: Automation of radiation treatment planning. III. A simplified system of digitising isodoses and direct print-out of dose distribution, Brit. J. Radiol. 36 (1963), 522—527.
29) Sterling, T.D., Perry, H., and Katz, L.: Automation of radiation treatment planning. IV. Derivation of a mathematical expression for the per cent depth dose surface of cobalt 60 beams and visualisation of multiple field dose distributions, Brit. J. Radiol. 37 (1964), 544—550.
30) Sterling, T.D., Perry, H., and Weinkam, J.J.: Automation of radiation treament planning. V. Calculation and visualisation of the total treatment volume. Brit. J. Radiol. 38 (1965), 906—913.
31) Sundbom, L.: Individually designed filters in cobalt 60 teletherapy, Acta Radiologica, Therapy, Physics,

Biology. 2 (1964), 189—208.
32) Tsien, K.C.: The application of automatic computing machines to radiation treatment planning, Brit. J. Radiol. 28 (1955), 432— 439.
33) Tsien, K.C.: A study of basic external radiation treatment techniques with the aid of automatic computing machines, Brit. J. Radiol. 31 (1958), 32—40.
34) Van de Geijn, J.: The computation of two and three dimensional dose distributions in cobalt 60 teletherapy, Brit. J. Radiol. 38 (1965), 369—377.
35) Wood, R.G.: The computation of dose distributions in cobalt rotational therapy, Brit. J. Radiol. 35 (1962), 482—484.